

**AFRL-ML-WP-TR-2003-4103**

**THE REPAIR OF SINGLE CRYSTAL  
NICKEL SUPERALLOY TURBINE  
BLADES USING LASER ENGINEERED  
NET SHAPE (LENS™) TECHNOLOGY**



**Michael G. Glavicic**

**UES, Inc.  
4401 Dayton-Xenia Rd.  
Dayton, OH 45432-1894**

**K.A. Sargent**

**AFRL/PRTC**

**P.A. Kobryn and S.L. Semiatin**

**AFRL/MLLMP**

**JANUARY 2003**

**Interim Report for 05 January 2001 – 31 January 2003**

**Approved for public release; distribution is unlimited.**

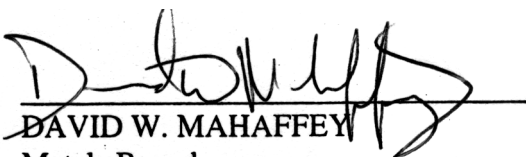
**MATERIALS AND MANUFACTURING DIRECTORATE  
AIR FORCE RESEARCH LABORATORY  
AIR FORCE MATERIEL COMMAND  
WRIGHT-PATTERSON AIR FORCE BASE, OH 45433-7750**

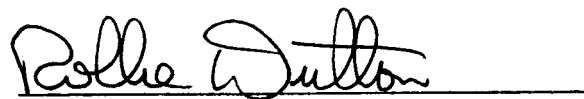
## NOTICE


WHEN GOVERNMENT DRAWINGS, SPECIFICATIONS, OR OTHER DATA ARE USED FOR ANY PURPOSE OTHER THAN IN CONNECTION WITH A DEFINITELY GOVERNMENT-RELATED PROCUREMENT, THE UNITED STATES GOVERNMENT INCURS NO RESPONSIBILITY OR ANY OBLIGATION WHATSOEVER. THE FACT THAT THE GOVERNMENT MAY HAVE FORMULATED OR IN ANY WAY SUPPLIED THE SAID DRAWINGS, SPECIFICATIONS, OR OTHER DATA, IS NOT TO BE REGARDED BY IMPLICATION OR OTHERWISE IN ANY MANNER CONSTRUED, AS LICENSING THE HOLDER OR ANY OTHER PERSON OR CORPORATION, OR AS CONVEYING ANY RIGHTS OR PERMISSION TO MANUFACTURE, USE, OR SELL ANY PATENTED INVENTION THAT MAY IN ANY WAY BE RELATED THERETO.

THIS REPORT IS RELEASABLE TO THE NATIONAL TECHNICAL INFORMATION SERVICE (NTIS). AT NTIS, IT WILL BE AVAILABLE TO THE GENERAL PUBLIC, INCLUDING FOREIGN NATIONS.

THIS TECHNICAL REPORT HAS BEEN REVIEWED AND IS APPROVED FOR PUBLICATION.

  
DAVID W. MAHAFFEY  
Metals Branch  
Metals, Ceramics & NDE Division

  
ROLLIE E. DUTTON, Chief  
Metals Branch  
Metals, Ceramics & NDE Division

  
GERALD J. PETRAK, Asst Chief  
Metals, Ceramics & NDE Division  
Materials and Manufacturing Directorate

IF YOUR ADDRESS HAS CHANGED, IF YOU WISH TO BE REMOVED FROM OUR MAILING LIST, OR IF THE ADDRESSEE IS NO LONGER EMPLOYED BY YOUR ORGANIZATION, PLEASE NOTIFY, AFRL/MLLMP, WRIGHT-PATTERSON AFB, OH 45433-7750 TO HELP US MAINTAIN A CURRENT MAILING LIST.

COPIES OF THIS REPORT SHOULD NOT BE RETURNED UNLESS RETURN IS REQUIRED BY SECURITY CONSIDERATIONS, CONTRACTUAL OBLIGATIONS, OR NOTICE ON A SPECIFIC DOCUMENT.

<b>REPORT DOCUMENTATION PAGE</b>					<i>Form Approved</i> <i>OMB No. 0704-0188</i>	
The public reporting burden for this collection of information is estimated to average 1 hour per response, including the time for reviewing instructions, searching existing data sources, gathering and maintaining the data needed, and completing and reviewing the collection of information. Send comments regarding this burden estimate or any other aspect of this collection of information, including suggestions for reducing this burden, to Department of Defense, Washington Headquarters Services, Directorate for Information Operations and Reports (0704-0188), 1215 Jefferson Davis Highway, Suite 1204, Arlington, VA 22202-4302. Respondents should be aware that notwithstanding any other provision of law, no person shall be subject to any penalty for failing to comply with a collection of information if it does not display a currently valid OMB control number. <b>PLEASE DO NOT RETURN YOUR FORM TO THE ABOVE ADDRESS.</b>						
<b>1. REPORT DATE (DD-MM-YY)</b> January 2003		<b>2. REPORT TYPE</b> Interim		<b>3. DATES COVERED (From - To)</b> 01/05/2001 – 01/31/2003		
<b>4. TITLE AND SUBTITLE</b> THE REPAIR OF SINGLE CRYSTAL NICKEL SUPERALLOY TURBINE BLADES USING LASER ENGINEERED NET SHAPE (LENS™) TECHNOLOGY				<b>5a. CONTRACT NUMBER</b> F33615-00-C-5212		
				<b>5b. GRANT NUMBER</b>		
				<b>5c. PROGRAM ELEMENT NUMBER</b> 62102F		
<b>6. AUTHOR(S)</b> Michael G. Glavicic (UES) K.A. Sargent (AFRL/PRTC) P.A. Kobryn and S.L. Semiatin (AFRL/MLLMP)				<b>5d. PROJECT NUMBER</b> 4347		
				<b>5e. TASK NUMBER</b> 25		
				<b>5f. WORK UNIT NUMBER</b> 02		
<b>7. PERFORMING ORGANIZATION NAME(S) AND ADDRESS(ES)</b>  <div style="display: flex; justify-content: space-between;"> <div style="width: 30%;">           UES, Inc.            4401 Dayton-Xenia Rd.            Dayton, OH 45432-1894         </div> <div style="width: 30%;">           AFRL/PRTC             AFRL/MLLMP         </div> </div>				<b>8. PERFORMING ORGANIZATION REPORT NUMBER</b>		
<b>9. SPONSORING/MONITORING AGENCY NAME(S) AND ADDRESS(ES)</b> Materials and Manufacturing Directorate Air Force Research Laboratory Air Force Materiel Command Wright-Patterson AFB, OH 45433-7750				<b>10. SPONSORING/MONITORING AGENCY ACRONYM(S)</b> AFRL/MLLMP		
				<b>11. SPONSORING/MONITORING AGENCY REPORT NUMBER(S)</b> AFRL-ML-WP-TR-2003-4103		
<b>12. DISTRIBUTION/AVAILABILITY STATEMENT</b> Approved for public release; distribution is unlimited.						
<b>13. SUPPLEMENTARY NOTES</b> Report contains color.						
<b>14. ABSTRACT</b> A feasibility study to evaluate Laser Engineered Net Shape (LENS™) technology as a general repair vehicle for single-crystal nickel superalloy turbine blades was conducted. A variety of deposition conditions at several locations were examined. The crystallographic orientation and microstructures of the deposits and substrates were examined using a scanning electron microscope (SEM) equipped to collect Electron-Back-Scatter-Diffraction (EBSD) data. The results of this study indicated that, for a variety of deposition conditions, it was possible to produce deposits that had the same crystallographic orientation as the substrate. The main difficulties encountered were the development of cracks in the deposits and the unreliability of the LENS™ system used.						
<b>15. SUBJECT TERMS</b> nickel, superalloys, turbine blades, single crystal						
<b>16. SECURITY CLASSIFICATION OF:</b>			<b>17. LIMITATION OF ABSTRACT:</b> SAR	<b>18. NUMBER OF PAGES</b> 28	<b>19a. NAME OF RESPONSIBLE PERSON (Monitor)</b> David W. Mahaffey <b>19b. TELEPHONE NUMBER (Include Area Code)</b> (937) 255-9840	
<b>a. REPORT</b> Unclassified	<b>b. ABSTRACT</b> Unclassified	<b>c. THIS PAGE</b> Unclassified				

# TABLE OF CONTENTS

<u>Section</u>	<u>Page</u>
<b>LIST OF FIGURES .....</b>	<b>iv</b>
<b>LIST OF TABLES .....</b>	<b>v</b>
<b>FOREWORD .....</b>	<b>vi</b>
<b>ACKNOWLEDGEMENTS .....</b>	<b>vi</b>
<b>1 INTRODUCTION .....</b>	<b>1</b>
<b>2 EXPERIMENTAL PROCEDURES .....</b>	<b>2</b>
2.1 MATERIAL .....	2
2.2 EXPERIMENTAL PROCEDURE.....	3
<b>3 RESULTS .....</b>	<b>4</b>
3.1 INITIAL FEASIBILITY STUDY .....	4
3.2 PARAMETRIC VARIATION OF DEPOSITION PARAMETERS, $P^*$ , $V^*$ , AND $H^*$ .....	6
3.3 CONTROL OF THE THERMAL GRADIENT .....	11
3.4 DEPOSITIONS ON A TURBINE BLADE SURFACE.....	12
<b>4 CONCLUSION .....</b>	<b>16</b>
<b>5 REFERENCES.....</b>	<b>17</b>
<b>LIST OF ACRONYMS .....</b>	<b>18</b>

## List of Figures

<u>Figure</u>	<u>Page</u>
Figure 1. Single Crystal Blade Platform and Initial Feasibility Specimen 190-0: (a) [100] and (b) [001] Perspective .....	2
Figure 2. Preliminary Feasibility Specimen 190-0: (a) Crack in Deposit, (b) Change in Microstructure Prior to Crack Initiation, (c) Back-Scattered-Electron Image of Dendritic Colony Microstructure Along Crack Fault Line, (d) Secondary-Electron-Image of Crack Fault Line, (e) Grain Multiplication Prior to Crack Formation, and (f) Deposit Substrate Interface .....	5
Figure 3. EBSD Analysis of Specimen 190-0 at the Deposit Substrate Interface: (a) Back-Scattered-Electron Image, (b) Inverse Pole Figure Map, (c) Pole Figures, and (d) Inverse Pole Figures of Region Scanned .....	6
Figure 4: Photographs of Deposits Prior to Sectioning of Specimens Indicated in Table 3: (a) [100] Direction, and (b) [010] Direction .....	8
Figure 5: X-ray Radiographic Images of Deposits Prior to Sectioning of Specimens Indicated in Table 3 (Arrow Indicated Location of Crack): (a) [100] Direction, and (b) [010] Direction .....	9
Figure 6. Back-Scattered-Electron Images of Specimen 190-3: (a) Crack at Deposit Substrate Interface, and (b) Epitaxial Columnar Grain Growth Observed in Other Regions .....	10
Figure 7. Optical Photographs of Crack Formations Observed in Subset of Specimens from Table 4: (a) 5-7, (b) 5-8, (c) 5-0, and (d) 5-II.....	12
Figure 8. Deposition Trials on Main Surface of Turbine Blade: (a) Photograph of all Deposits Listed in Table 5, EBSD Analysis of Specimen (b) B-10, and (c) B-7 at Deposit Substrate Interface .....	14
Figure 9. Orientation of Columnar Growth in Relation to [010] Direction of Turbine Blade: (a) [010] Directions in Specimen B-7 (b) Columnar Growth Direction in Specimen B-7, (c) [100] Directions in Specimen B-10, and (d) Columnar Growth in Direction in Specimen B-10 .....	15

## List of Tables

<u>Table</u>	<u>Page</u>
Table 1. System Specific Deposition Parameters Used in Initial Feasibility Study.....	3
Table 2. Range of Deposition Parameters Used in Initial Parametric Study.....	7
Table 3. Subset of Specimens Selected From Table 2 That Had X-Ray Radiographic Images Taken Prior to Sectioning .....	8
Table 4. Deposition Parameters Selected in an Attempt to Maintain $\frac{G^h}{V} > K$ During the Entire Deposition.....	11
Table 5. Deposition Parameters Used in Turbine Blade Surface Trials.....	13

## **FOREWORD**

This report was prepared by the Materials and Processes Division of UES, Inc., Dayton, Ohio under Air Force Contract No. F33615-00-C-5212. Mr. D. W. Mahaffey of the Metals Branch of the Metals, Ceramics and Non-Destructive Evaluation Division of the Air Force Research Laboratory was the Government Project Engineer. The research reported herein covers the period 05 January 2001 to 31 January 2003.

## **ACKNOWLEDGEMENTS**

This work was conducted as part of the in-house research activities of the Metals Processing Group of the Air Force Research Laboratory's Materials and Manufacturing Directorate. The support and encouragement of the Laboratory management and the Air Force Office of Scientific Research (Dr. C. S. Hartley, program manager) are gratefully acknowledged. One of the authors (MGG) was supported through Air Force Contract F33615-00-C-5212.

## INTRODUCTION

In modern gas turbine designs, single crystal turbine blades are typically used in place of directionally solidified and equiaxed parts. The introduction of single crystal blades into these engine designs allows the engines to operate at a higher temperature, improving their overall efficiency. In addition, the lack of grain boundaries in these parts also improves their creep resistance and thermal fatigue behavior [1, 2]. The main drawback of implementing this technology is the replacement cost of cracked or damaged blades. As a result, it is of great interest to develop new techniques to repair single crystal parts.

In the past epitaxial laser metal forming (E-LMF) has been investigated as a repair vehicle of cracks that occur in the platform of the turbine blade [3,4]. In this process a laser is focused on the surface of a part to be repaired and stream of metallic powder is then injected into the focal point of the laser. The laser then traverses the repair region forming a deposit whose shape is characteristic of the raster pattern.

Microstructural processing maps, which describe the transition between a columnar grain structure to equiaxed grains have also been developed for the E-LMF process [4]. In these maps the microstructure developed is described by

$$\frac{G^h}{V} = a \left\{ \sqrt[3]{\frac{-4pN_0}{3 \ln[1-f]}} \frac{1}{h+1} \right\}^h \quad (1)$$

in which  $G$  is the thermal gradient,  $V$  is the solidification velocity,  $N_0$  is the number of nucleation sites,  $f$  is the volume fraction of equiaxed grains and  $a$  and  $\eta$  are material dependant parameters. According to Hunt [5] when the volume fraction of equiaxed grains  $\phi > 0.49$  a fully equiaxed grain microstructure will occur and when  $\phi < 0.0066$  a fully columnar microstructure occurs. Using  $f = 0.0066$  as an upper bound for a columnar microstructure to develop in Equation 1, a bounding expression for the development of a columnar microstructure can be derived

$$\frac{G^h}{V} > K \quad (2)$$

in which  $K$  is a material dependant constant.

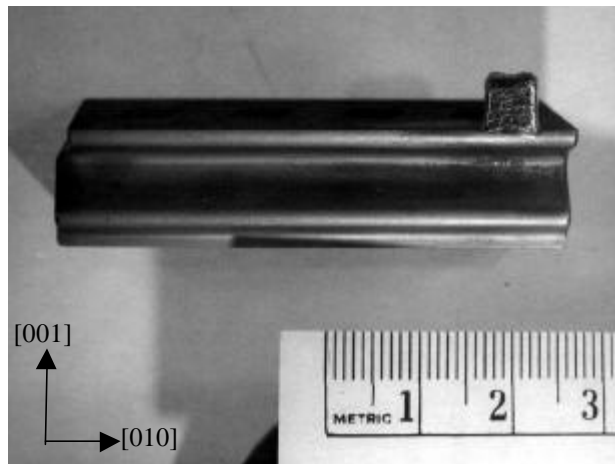
A completely analogous commercial process with a different trademark acronym is the laser engineered net shaping (LENS™) process. Because the LENS™ technique is analogous to E-LMF, it should also obey Equation 2. For this reason, a feasibility study was conducted to determine whether the parameters for the repair of RENE N5 single crystal turbine blades using LENS™ could be determined by trial and error in conjunction with Equation 2. In addition, the affects of surface preparation, surface geometry and crystallographic orientation on the deposit formed were also examined.



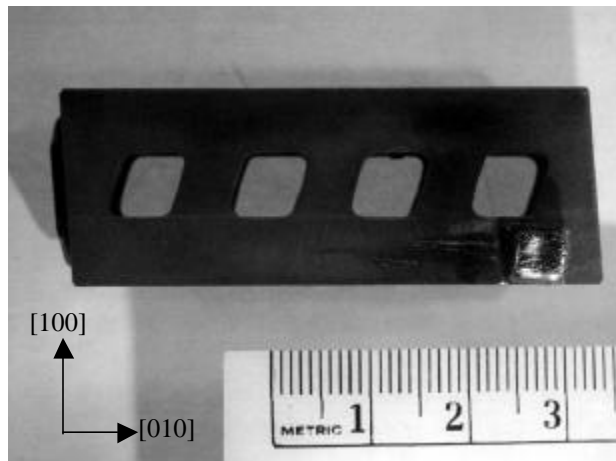
## EXPERIMENTAL PROCEDURES

### 1.1 Material

The depositions were performed on Rene N5 single crystal turbine blades using 45 to 150  $\mu\text{m}$  particle size Rene N5 powder purchased from Nuclear Metals Inc. Depositions were conducted on the main surface as well as the dovetail platform of the directionally solidified single crystal turbine blades. The dovetail platforms, Figure 1, were revealed by the removal of the main blade using an electronic discharge machine (EDM).



(a)



(b)

Figure 1. Single Crystal Blade Platform and Initial Feasibility Specimen 190-0: (a) [100] and (b) [001] Perspective

## 1.2 Experimental Procedure

The depositions were performed on an Optomec LENS™ 750 system with a 1000W Lumonics Nd: YAG laser focused to a spot size of 0.5mm. The system specific control parameters used in this work are given in Table 1. Three differently prepared main surfaces were used as deposition substrates: an as EDM surface, an EDM surface ground up to an 800-grit finish, and an EDM surface polished to a 1  $\mu\text{m}$  diamond finish. The turbine blade surface depositions were performed after the surface had been ground to an 800-grit finish. All depositions were configured in either a 5-mm by 5-mm square pattern or a single 5-mm-line pattern. For square deposits, when several layers were to be successively laid down on top of one another, a crosshatch pattern, which involved the rotation of the specimen by 60 degrees between successive depositions, was sometimes performed.

Table 1. System Specific Deposition Parameters Used in Initial Feasibility Study

Deposition Parameters	
Laser Power (P*)	35A, 280W
Hatch Space	0.15"
Layer Thickness (H*)	.01
Contours	1
Beam Offset	0
Acceleration	60000
Laser on Feed Rate (V*)	25"/min.
Powder Feed	3.95 V
Mass Flow Argon	3.33
Oxygen (ppm)	5
Hatch Angle	60°
Hatch Shrink	0.006
Contour Offset	0
Shutter Delay	20 ms
Deceleration	600000
Laser Off Feed Rate	60"/min.
Rpm	6.0
Center Purge	40

All specimens were prepared for electron-back-scatter-diffraction (EBSD) analysis using standard metallographic techniques. The EBSD measurements were performed using a Leica Cambridge Stereoscan 360 FE scanning electron microscope (SEM) with a Noran Voyager EBSD data-collection system and Tex Sem Laboratory (TSL) version 2.6 orientation imaging microscopy (OIM) software. The x-ray radiographic images were collected using a Phillips 160 operated at a power of 160 kV and 10 mA with an exposure time between 2 and 5 minutes.

## RESULTS

The results compiled in this report represent an amalgamation of several trials where deposition parameters were selected on the basis of the results of a previous trial. For this reason the results in this report will be laid out in several sections that represent the chronological order in which they were performed.

### 1.3 Initial Feasibility Study

Specimen 190-0 was a preliminary specimen that was used to establish whether an expanded set of depositions of Ni onto the dovetails of jet engine turbine blades was warranted. A total of sixteen layers were laid down using the parameters shown in Table 1 into an unprepared surface that had the turbine blade region removed (Figure 1) using EDM. Micrographs of the resultant deposit were taken after sectioning to examine its interior.

Examination of the interior of the specimen [Figure 2(a)] revealed that a large crack had developed in the deposit. Out of a total of sixteen layers, the crack extended from the top surface to the middle region of the third layer. In addition, several swirling patterns can be seen within a layer, which were attributed to the partial re-melting of the microstructure during deposition of subsequent layers at different crosshatch angles.

Higher magnification photographs of the deposit showed that in regions where a crack had appeared [Figure 2(b)], the columnar layering was interrupted by a more globular type of equiaxed grain structure just prior to the formation of a crack. Based upon Equation 2, the cracking phenomenon appeared to have occurred immediately after to the transition of  $\frac{G^h}{V}$  from a columnar growth regime to an equiaxed growth regime. As a result, it would then appear that, for Rene N5, the onset of cracking is also linked to a critical volume fraction of  $\phi = 0.0066$  being formed during deposition.

Further along the crack towards the top surface, a series of columnar colony microstructures were observed along the fault line, Figure 2(c), and Figure 2(d). The orientation of the columnar grains contained within these colonies, varied their orientation on the two opposing crack interfaces, which indicated that the crack was initiated and propagated during solidification.

In addition to the nucleation and growth of a critical volume fraction of equiaxed grains, other mechanisms such as Grain Multiplication were also correlated to the formation of cracks, Figure 2(e). In this process, dendrite arms were re-melted and then separated from the main dendrite. If the arm that is separated is then carried away in the slightly super-cooled liquid a new crystal is formed without a new nucleation event.

At the interface between the substrate and deposit, Figure 2(f), a crack free 3  $\mu\text{m}$  wide columnar microstructure was formed. EBSD analysis of this region, Figure 3, indicated that the crystallographic orientation of the deposit was the same as the substrate. More over the growth direction of the dendrites observed was parallel to the [001] crystallographic direction in the

substrate, which is consistent with the known growth mechanism of dendrites in face-centered cubic materials.

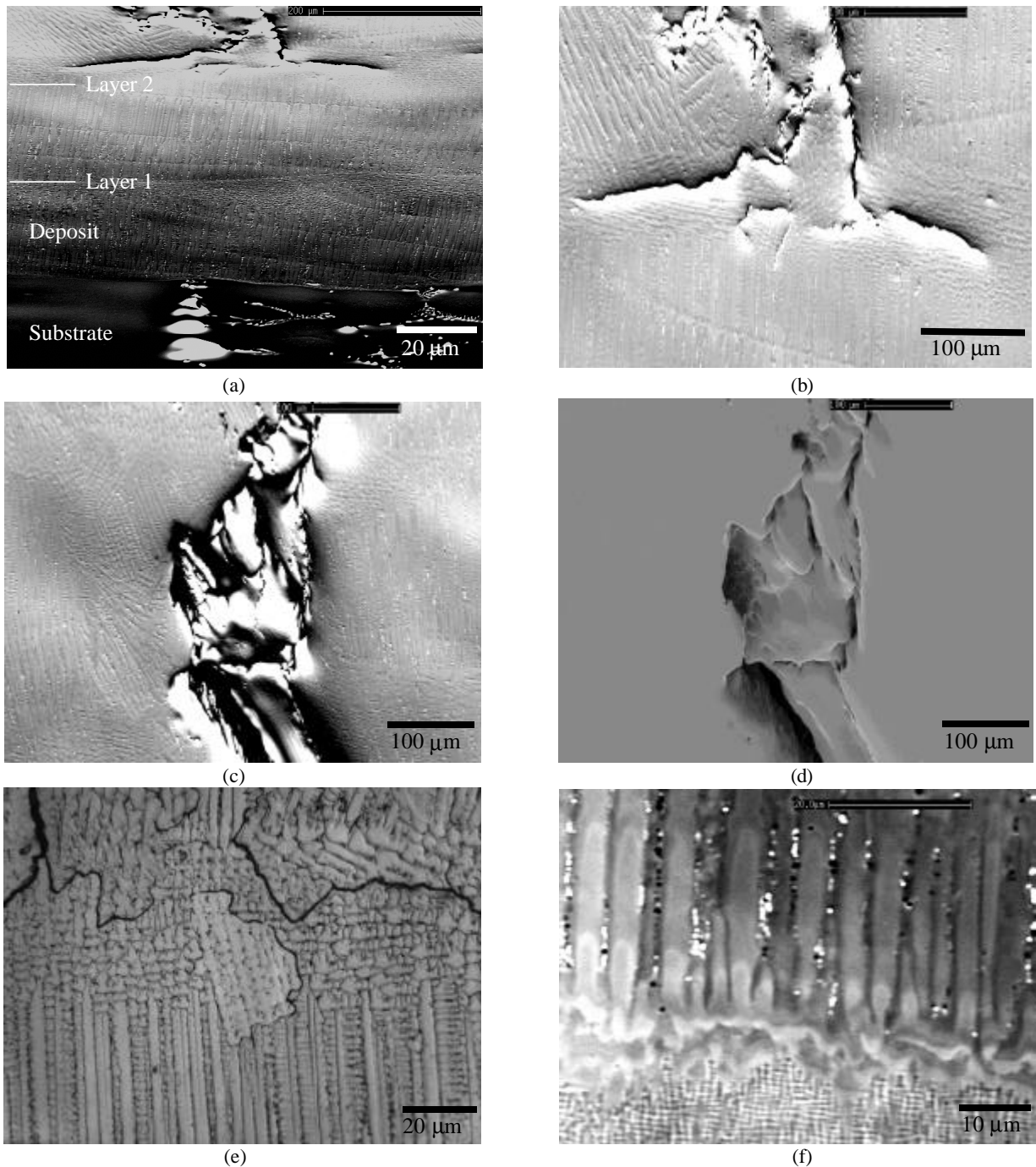


Figure 2. Preliminary Feasibility Specimen 190-0: (a) Crack in Deposit, (b) Change in Microstructure Prior to Crack Initiation, (c) Back-Scattered-Electron Image of Dendritic Colony Microstructure Along Crack Fault Line, (d) Secondary-Electron-Image of Crack Fault Line, (e) Grain Multiplication Prior to Crack Formation, and (f) Deposit Substrate Interface

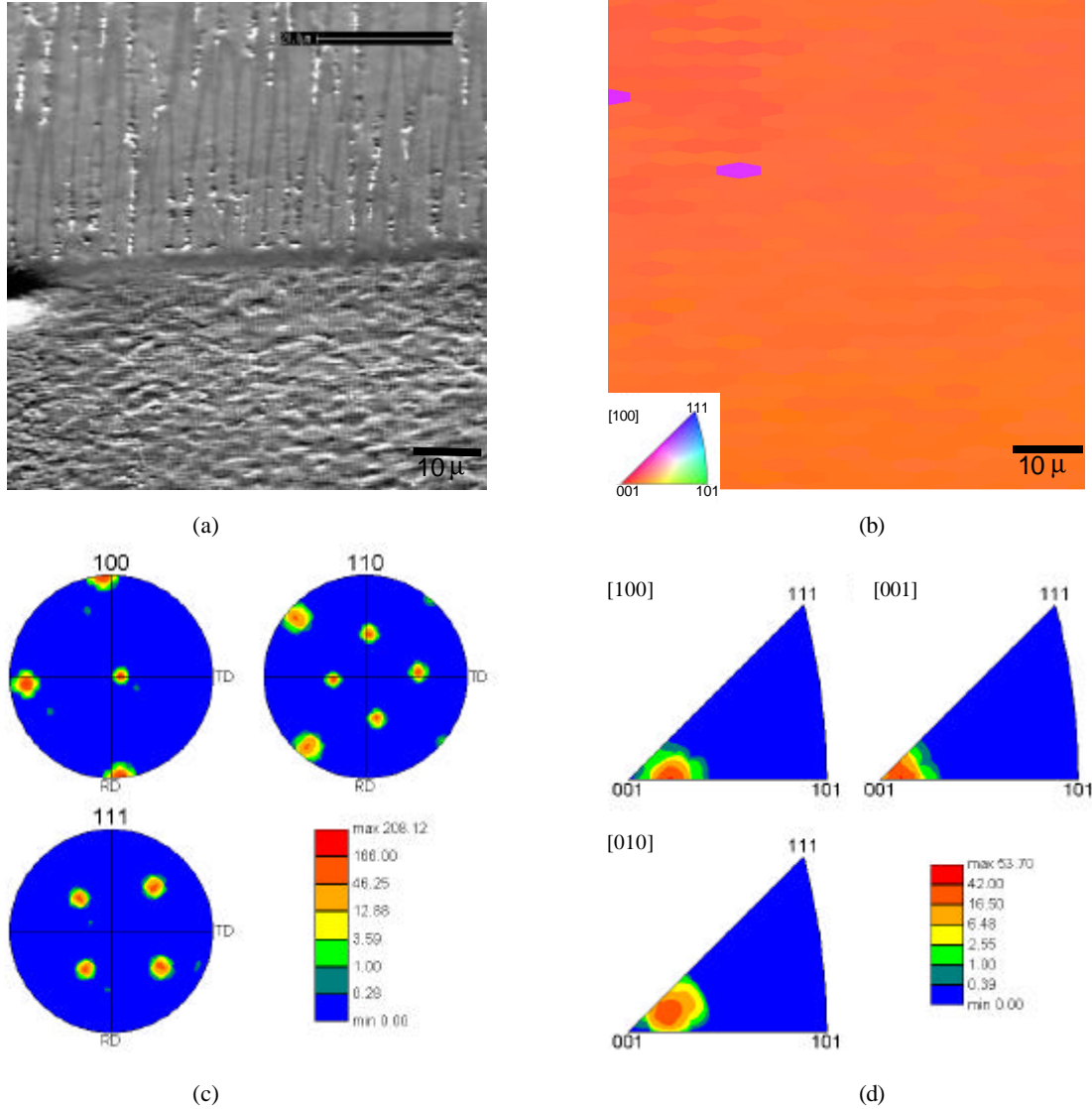


Figure 3. EBSD Analysis of Specimen 190-0 at the Deposit Substrate Interface: (a) Back-Scattered-Electron Image, (b) Inverse Pole Figure Map, (c) Pole Figures, and (d) Inverse Pole Figures of Region Scanned

#### 1.4 Parametric Variation of Deposition Parameters, $P^*$ , $V^*$ , and $H^*$

Because the deposition parameters initially selected,  $P^*$ ,  $V^*$  and  $H^*$ , were selected to optimize the shape of the deposit, a second set of depositions, Table 2, were carried out where the affects of surface finish and deposition parameters were evaluated. In order to conclusively prove that the cracking phenomenon observed in specimen 190-0 had occurred during deposition and not during the subsequent sample preparation, a subset of the specimens which represented the range of parametric variations examined, Table 3, had photographs, Figure 4, and x-ray radiographic images, Figure 5, taken prior to sectioning. Of the seven selected, large cracks were clearly visible in the radiographs of six. All six cracks were also only visible in the [100] direction of the single crystal substrate, which indicated a directional dependence in their formation. The origin

of this dependence may be attributed to the differences in the shape of the underlying substrate in the [100], and [010] directions, Figure 5.

Table 2. Range of Deposition Parameters Used in Initial Parametric Study

Specimen	Surface Prep.	Location No.	Power	Velocity	Deposition Type	Build Height	Layers	Cross Hatched
5	EDM + Ground + Polish	1	P*	V*	5 x 5 mm	H*	Laser Glaze	Yes
		2	P*	V*	5 x 5 mm		1	Yes
		3	P*	V*	5 x 5 mm		2	Yes
		4	P*	V*	5 x 5 mm		4	Yes
		5	P*	V*	5 x 5 mm		8	Yes
		6	P*	V*	5 x 5 mm		16	Yes
		1	P*	V*	5 x 5 mm		Laser Glaze	Yes
34	EDM + Ground	2	P*	V*	5 x 5 mm	H*	1	Yes
		3	P*	V*	5 x 5 mm	H*	2	Yes
		4	P*	V*	5 x 5 mm	H*	4	Yes
		5	P*	V*	5 x 5 mm	H*	8	Yes
		6	P*	V*	5 x 5 mm	H*	16	Yes
		1	P*	V*	5 x 5 mm	H*	Laser Glaze	Yes
68	EDM	2	P*	V*	5 x 5 mm	H*	1	Yes
		3	P*	V*	5 x 5 mm	H*	2	Yes
		4	P*	V*	5 x 5 mm	H*	4	Yes
		5	P*	V*	5 x 5 mm	H*	8	Yes
		6	P*	V*	5 x 5 mm	H*	16	Yes
		7	P*	V*	5 x 5 mm	H*	3	No
		8	P*	V*	5 x 5 mm	H*	16	No
		9	P*	V*	5 x 5 mm	H*/2	16	Yes
		0	P*	V*	5 x 5 mm	H*	16	Yes
		1	P*	1.25V*	5 x 5 mm	H*	16	Yes
		2	P*	1.50V*	5 x 5 mm	H*	16	Yes
190	EDM	3	1.50P*	V*	5 x 5 mm	H*	16	Yes
		4	P*	V*	5-mm Line	H*	1	No
		5	P*	V*	5-mm Line	H*	4	No
		6	P*	V*	5-mm Line	H*	16	No

Upon sectioning, specimen 190-3, which showed no evidence of cracking in the radiographic photographs (Figure 5), revealed that a cluster of cracks had unfortunately formed in the central region of the specimen, Figure 6(a). The orientation of the crack surface was also in the [100] substrate direction, but these cracks did not extend to the upper layers of the deposit. At other regions along the interface region, a crack free columnar structure was seen, Figure 6(b). Overall, the severity of the cracking observed in specimen 190-3 was somewhat less than that of the remaining specimens.



Table 3. Subset of Specimens Selected From Table 2 That Had X-Ray Radiographic Images Taken Prior to Sectioning

Specimen	Surface Prep.	Location No.	Power	Velocity	Build Height	Cross Hatched
68	EDM	6	P*	V*	H*	Yes
68	EDM	8	P*	V*	H*	No
68	EDM	9	P*	V*	½ H*	Yes
190	EDM	1	P*	1.25V*	H*	Yes
190	EDM	2	P*	1.5V	H*	Yes
190	EDM	3	1.5P*	V*	H*	Yes
5	EDM + Ground + Polish	6	P*	V*	H*	Yes

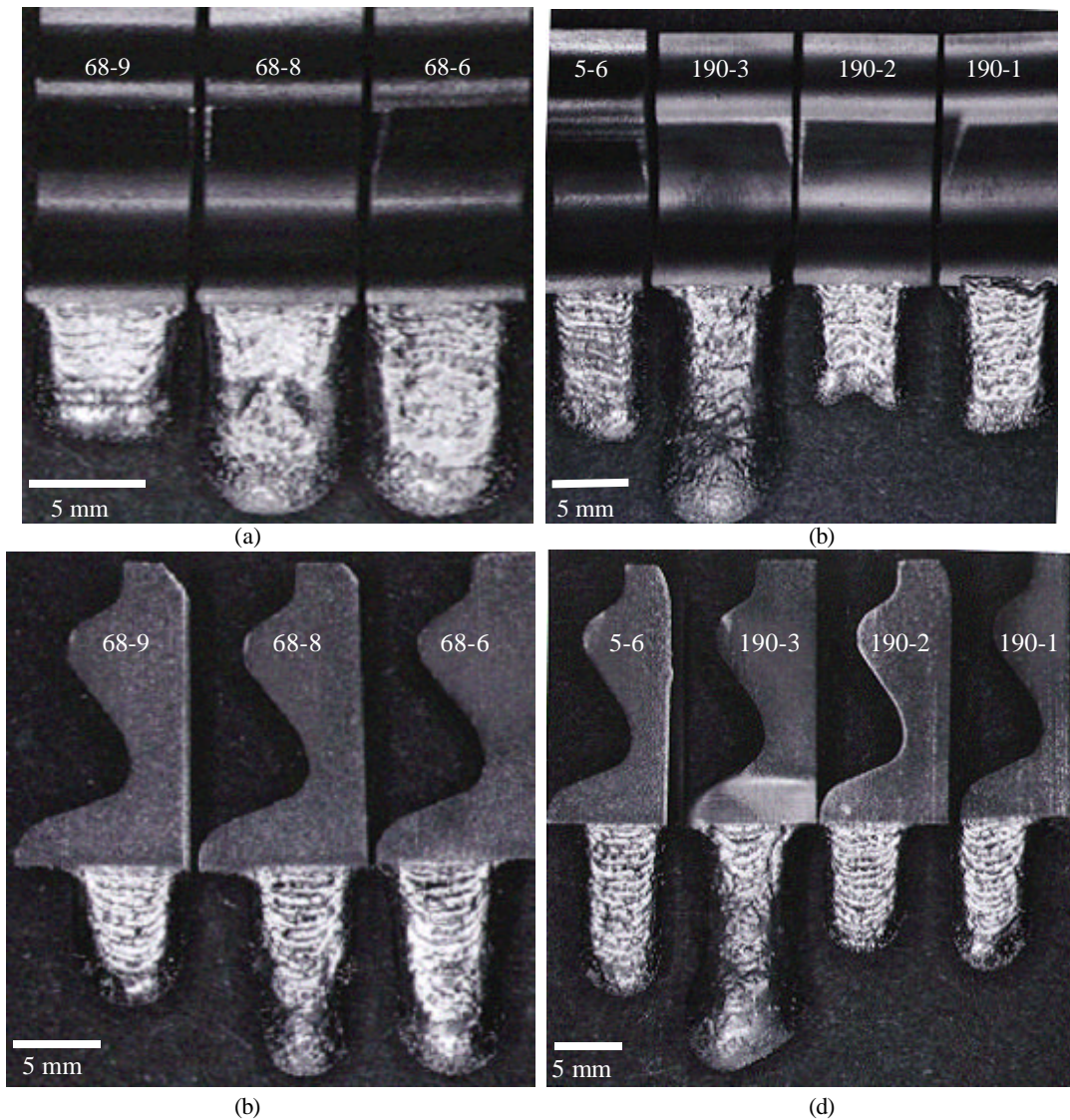
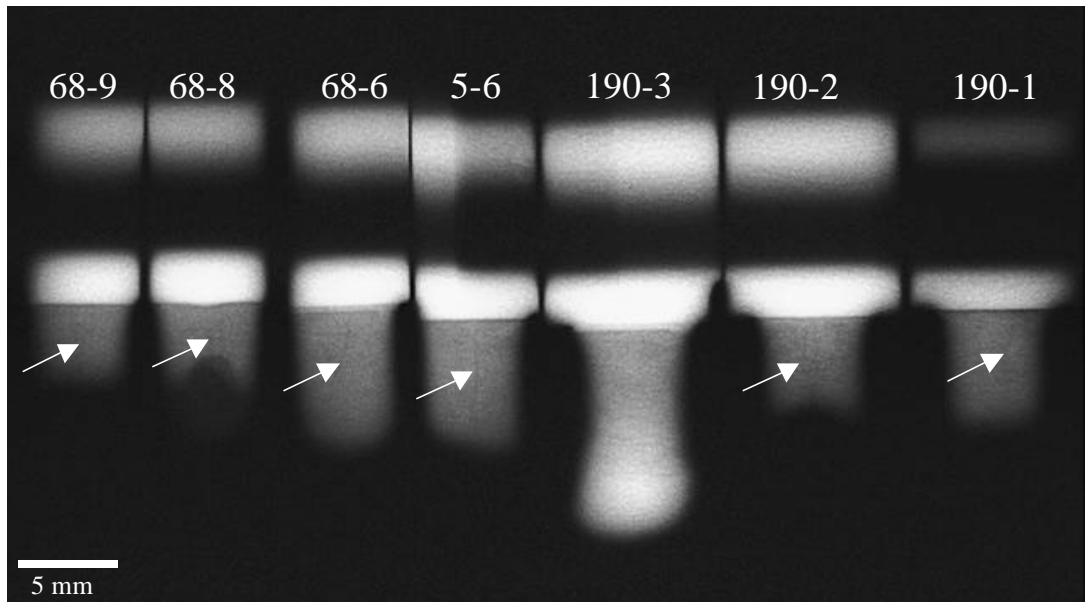
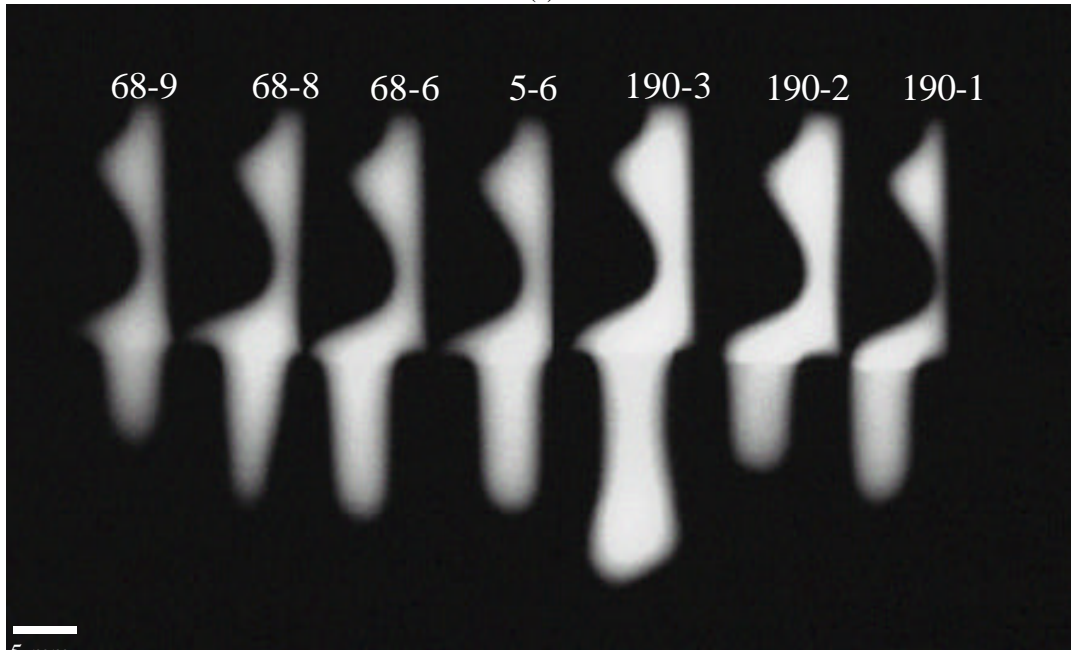


Figure 4: Photographs of Deposits Prior to Sectioning of Specimens Indicated in Table 3: (a) [100] Direction, and (b) [010] Direction



(a)



(b)

Figure 5: X-ray Radiographic Images of Deposits Prior to Sectioning of Specimens Indicated in Table 3 (Arrow Indicated Location of Crack): (a) [100] Direction, and (b) [010] Direction



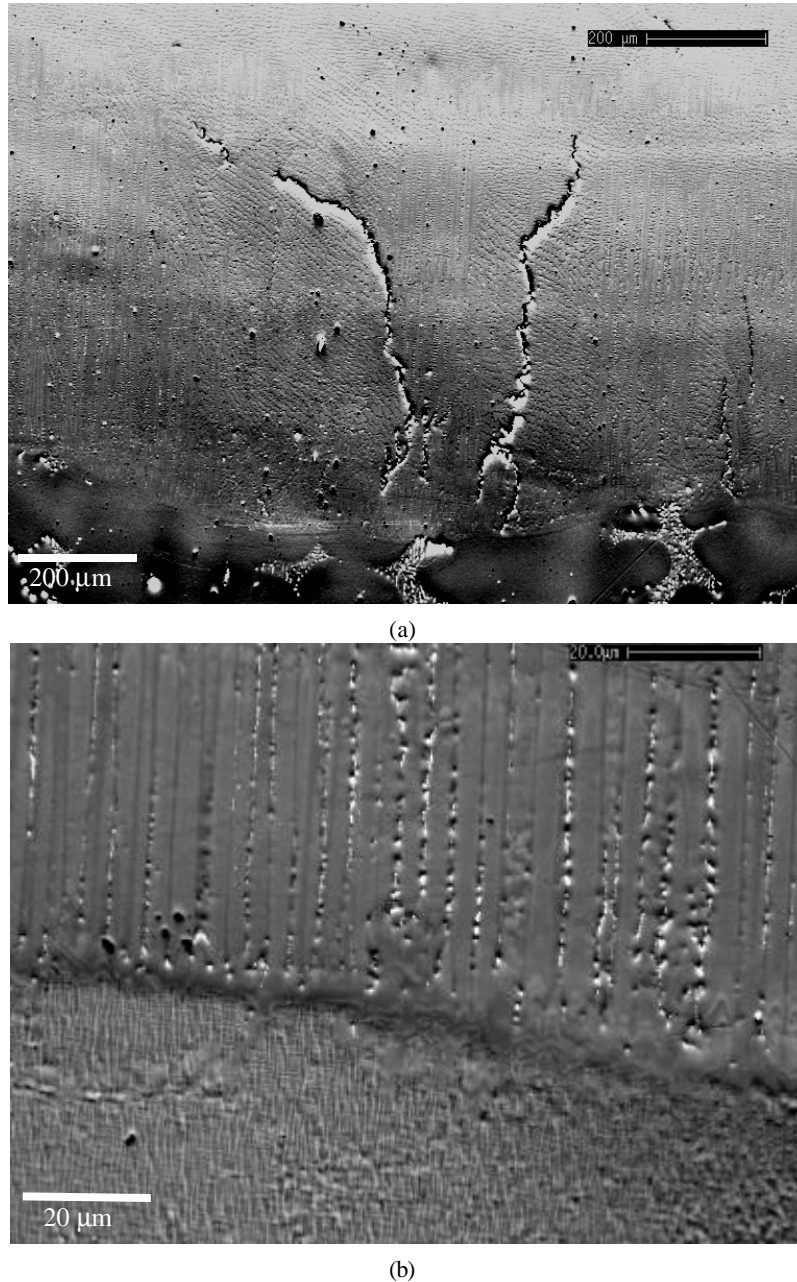


Figure 6. Back-Scattered-Electron Images of Specimen 190-3: (a) Crack at Deposit Substrate Interface, and (b) Epitaxial Columnar Grain Growth Observed in Other Regions

Inspection of the overall shapes of these deposits, Figure 4, showed that the variation of the deposition parameters could also have an adverse effect on the shape obtained. In particular, specimen 68-8, where no cross hatch was employed, formed a deposit whose shape was by no means uniform. A cusp in the deposit could be seen in both the radiographic image and photograph of this specimen. Variation of the laser power,  $P^*$ , and specimen translation velocity,  $V^*$  (specimens, 190-3, and 190-2 respectively), during deposition also affected the effective

build height and shape of the deposit formed even though the build height parameter  $H^*$  selected, was intended to remain the same.

Specimen 5-6 confirmed that the cracking phenomenon observed was not an artifact of depositing onto the as EDM surface since it too had cracks visible even though its surface had also been both ground and polished prior to deposition.

## 1.5 Control of the Thermal Gradient

Because cracking was observed in some of the deposits after several layers had been laid down onto the substrate, it was decided that the key to inhibit cracking may be to control the temperature of the substrate in some fashion so that the ratio  $\frac{G^h}{V}$  would stay well above the threshold for the formation of equiaxed grains and cracking. The simplest method to accomplish this task was to allow a dwell time in between the deposition of layers, and/or to preheat the substrate prior to deposition. A 400 °C substrate temperature was the maximum possible that could be obtained with the apparatus and for this reason alone this temperature was chosen to provide the maximum possible variation in the experiments performed, Table 4. All depositions in Table 4 were performed on the remaining regions of unpolished as EDM sectioned surfaces because surface preparation was determined to not affect the properties of the deposit.

Sectioning of the specimens revealed that once again all specimens had cracks in the deposit, Figure 7. In general the cracking problem in these trials was much more severe than that observed in the previous campaign. This was an unexpected result because the previous results indicated that the range of values for  $P^*$ ,  $V^*$  and  $H^*$  used in the past trials could all produce deposits that were crack free for several layers. In this present trial, the cracking was more frequent and occurred in the interfacial region between the substrate and deposit. As a result, it is unclear how to proceed in this parametric study, in light that it is suspected that there are stability and reproducibility issues with the Optomec LENS™ system.

Table 4. Deposition Parameters Selected in an Attempt to Maintain  $\frac{G^h}{V} > K$  During the Entire Deposition

Specimen	Location	Power	Velocity	Build Height	Heated to 400 °C	Delay Time
34	7	$P^*$	$V^*$	$H^*$	No	1 min/layer
34	8	$P^*$	$V^*$	$H^*$	Yes	None
34	9	$P^*$	$V^*$	$H^*$	Yes	1 min/layer
34	10	$1.5P^*$	$V^*$	$H^*$	Yes	None
34	11	$1.5P^*$	$V^*$	$H^*$	Yes	1 min/layer
5	7	$1.5P^*$	$V^*$	$H^*$	No	1 min/layer
5	8	$P^*$	$1.5V^*$	$H^*$	No	1 min/layer
5	9	$P^*$	$1.5V^*$	$H^*$	Yes	None
5	10	$P^*$	$1.5V^*$	$H^*$	Yes	1 min/layer
5	11	$P^*$	$V^*$	$H^*/2$	Yes	1 min/layer

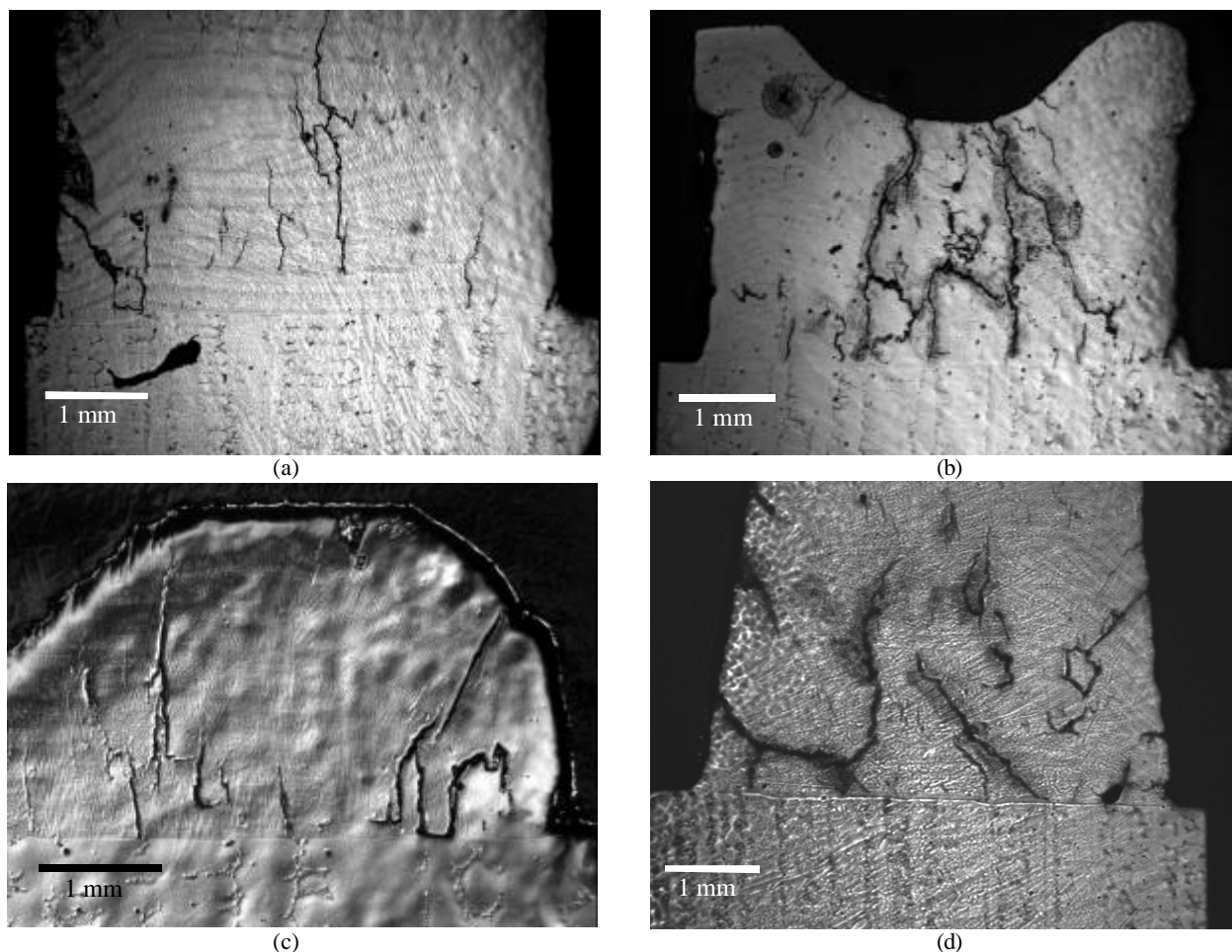


Figure 7. Optical Photographs of Crack Formations Observed in Subset of Specimens from Table 4: (a) 5-7, (b) 5-8, (c) 5-0, and (d) 5-11

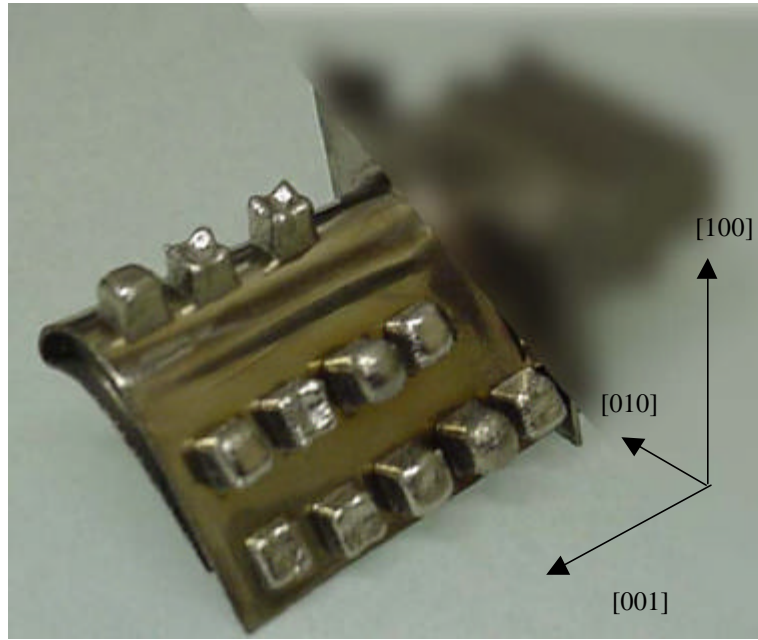
## 1.6 Depositions on a Turbine Blade Surface

The test matrix devised for the depositions onto the surface of an actual turbine blade are presented in Table 5. Two additional effects were also studied in this campaign, the affect of depositing onto a non-  $\{100\}$  single crystal with either a; flat or curved surface, Figure 8(a). In both cases the crystallographic orientation of the deposit in relation to the substrate were the same, Figure 8(b) and Figure 8(c), which indicated that it was possible to deposit at least one layer epitaxially on an arbitrarily oriented single crystal surface. The general shape of the deposits formed on the curved surface also indicated that some variation in the location of the focal spot of the laser in relation to the surface does not adversely affect the shape or crystallographic orientation of the deposit obtained and hence the repair of localized regions on a blade surface would not require the exact curvature of the blade to be known and followed during the repair.

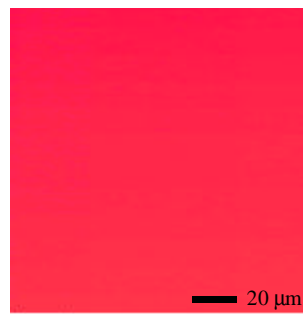
Table 5. Deposition Parameters Used in Turbine Blade Surface Trials

Specimen	Location	Power	Velocity	Build Height	Cross Hatched (60 °)	Heated to 400 °C	Delay Time
B-2	Flat Region	P*	V*	H*	Yes	No	1 min/layer
B-6	Flat Region	P*	V*	H*	Yes	Yes	None
B-7	Flat Region	P*	V*	H*	Yes	Yes	1 min/layer
B-3	Flat Region	1.5P*	V*	H*	Yes	No	1 min/layer
B-8	Flat Region	1.5P*	V*	H*	Yes	Yes	None
B-9	Flat Region	1.5P*	V*	H*	Yes	Yes	1 min/layer
B-4	Flat Region	1.5P*	V*	H*	Yes	No	None
B-5	Flat Region	P*	V*	H*	Yes	No	None
B-10	Curved Region	P*	V*	H*	Yes	No	None
B-12	Curved Region	P*	V*	H*	Yes	Yes	1 min/layer
B-11	Curved Region	P*	V*	H*	Yes	No	1 min/layer

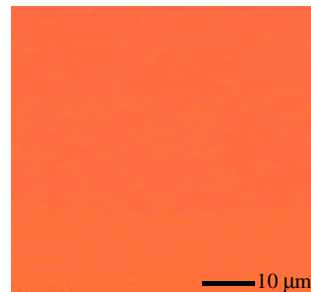
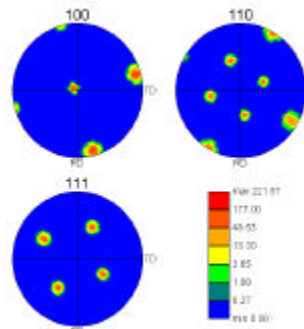
The microstructure of the deposits in relation to the crystallographic orientation of the substrate, Figure 9, indicated that the mechanism responsible for the epitaxial deposition onto non- {100} oriented substrates is related to both the local temperature gradient and crystallographic orientation of the substrate during solidification. During solidification it appeared that the columnar grains forming oriented themselves in a fashion that best matches both a <100> crystallographic direction in the substrate and the thermal gradient present during solidification.



(a)



(b)



(c)

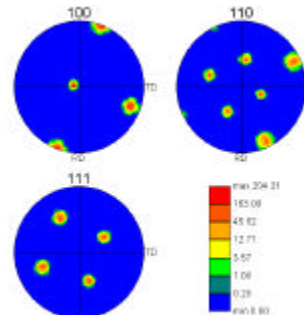


Figure 8. Deposition Trials on Main Surface of Turbine Blade: (a) Photograph of all Deposits Listed in Table 5, EBSD Analysis of Specimen (b) B-10, and (c) B-7 at Deposit Substrate Interface

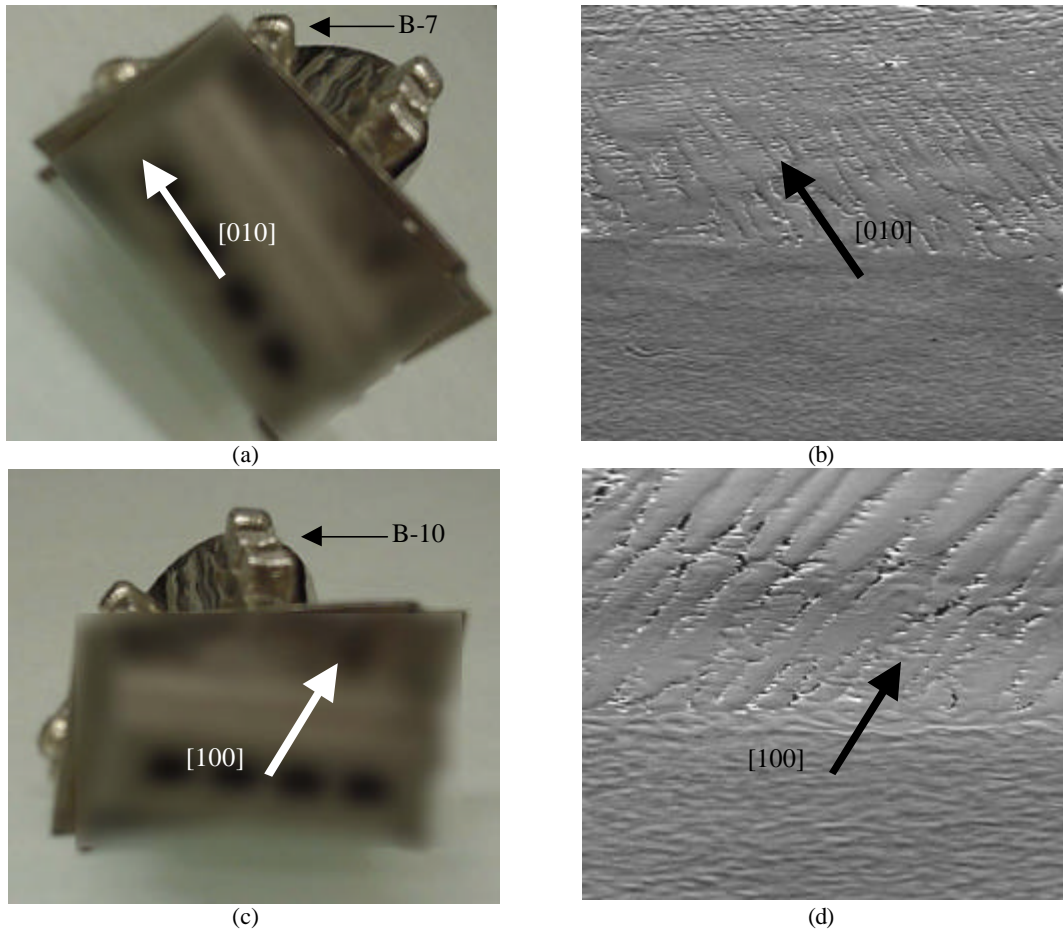


Figure 9. Orientation of Columnar Growth in Relation to [010] Direction of Turbine Blade: (a) [010] Directions in Specimen B-7 (b) Columnar Growth Direction in Specimen B-7, (c) [100] Directions in Specimen B-10, and (d) Columnar Growth in Direction in Specimen B-10

## CONCLUSION

Based upon the results obtained thus far in the project it would appear that the following conclusions could be drawn for the processing parameters employed:

1. In order to produce a specific shaped deposit, cross-hatching of the layers by 60 degrees is required.
2. The crystallographic orientation of the first few deposition layers is the same as that of the substrate regardless of the crystallographic orientation of the surface or the surface preparation procedures followed.
3. The orientation of the columnar grains at the substrate-deposit interface will orient themselves in a fashion that best matches the local temperature gradient and a  $\langle 100 \rangle$  crystallographic direction in the substrate.
4. Cracks are formed during solidification of the deposit.
5. The onset of cracking is linked to the onset of “Grain Multiplication” and an equiaxed microstructure being formed.
6. The Optomec LENS™ system used in these studies has some serious stability and reproducibility issues that are not understood at the present time.
7. It appears that if the stability and reproducibility issues with the LENS™ system can be solved, this technology may be a feasible repair vehicle for single crystal turbine blades.

## REFERENCES

1. E.A. Steigerwald, J. Mater. Educ. 16 (1994) 21.
2. G.L. Erickson, K. Harris, in: Coutsouradis, J.H. Davidson, J. Ewald, P. Greenfield, T. Khan, M. Malik, D.B. Meadowcroft, V. Regis, R.B. Scarlin, F. Schubert, D.V. Thorton (Eds.), Materials for Advanced Power Engineering, Kluwer Academic, Dordrecht, 1994, p. 1055.
3. M. Gäumann, S. Henry, F. Cléton, J.D. Wagnière, W. Kurtz, Mat. Sci. Eng. A271 (1999) 232.
4. M. Gäumann, C. Bezençon, P. Canalis, W. Kurtz, Acta Mater. 49 (2001) 1051.
5. J.D. Hunt, Mat. Sci. Eng. 65 (1984) 75.



## **LIST OF ACRONYMS**

<b>ACRONYM</b>	<b>DESCRIPTION</b>
AFRL/MLLM	Air Force Research Laboratory, Materials and Manufacturing Directorate
EBSD	Electron-back-scatter-diffraction
EDM	Electronic discharge machine
E-LMF	Epitaxial laser metal forming
LENS <sup>TM</sup>	Laser Engineered Net Shape
OIM	Orientation imaging microscopy
SEM	Scanning electron microscope
TSL	Tem Sem Laboratory